Received: 17 May 2023 | Revised: 9 September 2023 | Accepted: 9 October 2023

DOI: 10.1002/pld3.543

RESEARCH ARTICLE

Genome-wide identification and expression analysis of Na^+/H^+ *antiporter* (*NHX*) genes in tomato under salt stress

Erman Cavusoglu | **Ugur Sari** | **Iskender Tiryaki**

Department of Agricultural Biotechnology, Faculty of Agriculture, Canakkale Onsekiz Mart University, Terzioglu Campus, Canakkale, Turkey

Correspondence
Iskender Tiryaki, Department of Agricultural Biotechnology, Faculty of Agriculture, Canakkale Onsekiz Mart University, Terzioglu Campus, Canakkale 17020, Turkey.
Email: itiryaki@comu.edu.tr; tiryaki46@yahoo.com

Funding information
The open access publishing of this paper was funded by the Scientific and Technological Research Council of Turkey (TUBITAK).

Abstract

Plant Na^+/H^+ *antiporter* (*NHX*) genes enhance salt tolerance by preventing excessive Na^+ accumulation in the cytosol through partitioning of Na^+ ions into vacuoles or extracellular transport across the plasma membrane. However, there is limited detailed information regarding the salt stress responsive *SlNHX*s in the most recent tomato genome. We investigated the role of this gene family's expression patterns in the open flower tissues under salt shock in *Solanum lycopersicum* using a genome-wide approach. A total of seven putative *SlNHX* genes located on chromosomes 1, 4, 6, and 10 were identified, but no ortholog of the *NHX5* gene was identified in the tomato genome. Phylogenetic analysis revealed that these genes are divided into three different groups. SlNHX proteins with 10–12 transmembrane domains were hypothetically localized in vacuoles or cell membranes. Promoter analysis revealed that *SlNHX6* and *SlNHX8* are involved with the stress-related MeJA hormone in response to salt stress signaling. The structural motif analysis of SlNHX1, −2, −3, −4, and −6 proteins showed that they have highly conserved amiloride binding sites. The protein–protein network revealed that SlNHX7 and SlNHX8 interact physically with Salt Overly Sensitive (SOS) pathway proteins. Transcriptome analysis demonstrated that the *SlNHX2* and *SlNHX6* genes were substantially expressed in the open flower tissues. Moreover, quantitative PCR analysis indicated that all *SlNHX* genes, particularly *SlNHX6* and *SlNHX8*, are significantly upregulated by salt shock in the open flower tissues. Our results provide an updated framework for future genetic research and development of breeding strategies against salt stress in the tomato.

KEYWORDS
gene expression, Na^+/H^+ *antiporter*, *NHX*, *Solanum lycopersicum*, salt stress

1 | INTRODUCTION

Salt stress is considered one of the most important abiotic stress factors that negatively affects plant growth and development and causes serious yield losses in important crop species (Deinlein et al., 2014; Nataraja & Parvathi, 2016). Global warming has accelerated as well as expanded the land that limits the planting of important crop species due to high levels of salinity, which are thought to affect more than

6% of existing farmland and about 20% of irrigated land around the world (Munns & Tester, 2008). The adverse effects of salt can vary, depending on the developmental stages of a plant such as germination, early growth, and flowering or seeding stages (Chandna et al., 2013). Salt stress could affect essential biological processes including photosynthesis, water relationship, and nutrient uptake (Parihar et al., 2015). High concentrations of salt in the soil initially cause slower growth by reducing leaf and root growth, and then it becomes toxic to plant cells, leading to physiological disorders and cell death (Munns, 1993; Parihar et al., 2015). Plants under salt stress conditions accumulate high concentrations of Na^+ and Cl^- ions in the chloroplasts, inhibiting photosynthesis and decreasing chlorophyll content (Chutipaijit et al., 2011; Zhang et al., 2005). Over time, increased Na^+ concentrations in plant tissues become toxic, and this toxicity directly affects intracellular K^+ homeostasis (Shabala & Cuin, 2008). A critical Na^+/K^+ ratio must be reached in the cell for effectiveness of many cytosolic enzyme activities (Mahajan et al., 2008). With an increase in the amount of Na^+ in the external environment, the entry of Na^+ ions into the cell also increases, whereas the uptake of K^+ ions into the cell decreases, and accordingly, the Na^+/K^+ balance is disturbed. This is because Na^+ competes with K^+ for the sites where the K^+ ion binds (Tester & Davenport, 2003). Because K^+ ions play a direct in activating enzymes and to neutralizing negative charges of proteins, cells need high concentrations of K^+ ions for the stabilization of protein synthesis (Harrewijn, 1979; Marschner, 1995; Pandolfi et al., 2012). Furthermore, some plants show a positive correlation between K^+ content and yield (Ashraf & McNeilly, 2004; Bandeh-hagh et al., 2008; Valiollah, 2013).

To date, it has been demostrated that many ion transporters play important roles in maintaining the pH and ion homeostasis of plant cells in the presence of salt stress (Hamamoto et al., 2015; Pardo et al., 2006; Ward et al., 2009; Yamaguchi et al., 2013). The *Na^+/H^+ antiporter* (*NHX*) gene family, a subfamily of ion transporters, plays an important role in salt stress tolerance by controlling cellular pH and Na^+ ion balance in plants (Brett et al., 2005; Van Zelm et al., 2020). The first plant *NHX1* gene was identified in *Arabidopsis thaliana* (Gaxiola et al., 1999). The *NHX* gene family in *A. thaliana* includes eight members, which are divided into three subgroups (Brett et al., 2005). The *AtNHX1* (*A. thaliana NHX1*), *−2*, *−3*, and *−4* are referred to as Vac class *NHX*s on the vacuole membranes (Aharon et al., 2003), whereas *AtNHX5* and *AtNHX6*, which are in the Endo class of *NHXs*, are located on the endosomal region (Bassil et al., 2011). The amiloride binding domain (FFIYLLPPI) is located at the N-terminal of TM3 (transmembrane-3), and this domain, known as an inhibitor of *NHX* activity, is a characteristic feature of vacuolar class *NHX* members (Counillon et al., 1993; Yamaguchi et al., 2003). The *AtNHX7* and *AtNHX8* are found in the plasma membranes (PMs) and are referred to as PM class (Shi et al., 2000). *AtNHX7* (*AtSOS1*) is regulated by *Serine/threonine Protein Kinase* (*SOS2*) and *Calcineurin B-like Calcium-Binding Protein* (*SOS3*) in the *Salt Overly Sensitive* (*SOS*) signaling pathway (Qiu et al., 2002). In response to salt stress, intracellular Ca^{2+} increases, which triggers the activation of the *SOS* signaling pathway (Manishankar et al., 2018). *SOS3* activates the *SOS2* protein kinase, and the *SOS2-SOS3* complex then activates *SOS1/NHX7* by phosphorylation to efflux Na^+ ions out of the cell (Halfter et al., 2000; Liu et al., 2000; Shi et al., 2003). Previous reports have documented six *NHX* genes in *Medicago truncatula* (Sandhu et al., 2018), nine *NHX* genes in *Capsicum annuum* (Luo et al., 2021), five *NHX* genes in *Beta vulgaris* (Wu et al., 2019), six *NHX* genes in *Vitis vinifera* (Ayadi et al., 2020), 10 *NHX* genes in *Glycine max* (Chen et al., 2015), eight *NHX* genes in *Populus trichocarpa* (Tian et al., 2017), 10 *NHX* genes in *Punica granatum* (Dong et al., 2021), and eight *NHX* genes in *Actinidia chinensis* were identified (Liu et al., 2023). Such variation among the *NHX* gene numbers of plant species indicated that gene duplications or loss events occurred during species evolution, which also provided an opportunity to expand the *NHX* gene family by generation functionally divert new genes (Huang et al., 2022).

As a member of the *Solanaceae* family, tomato (*Solanum lycopersicum*) is diploid with 2n = 24 chromosomes (Díez & Nuez, 2008). It is highly cultivated worldwide and contains invaluable components for human nutrition such as lycopene, β-carotene, and vitamin C (Clinton, 2005). Tomato plants exhibit premature cell senescence, accumulation of Na^+ in the leaves, and a decrease in photosystem II efficiency when exposed to salt stress (100-mM NaCl) (Ghanem et al., 2012). It has been reported that both leaf area and dry matter content as well as K^+/Na^+ ratio of tomato plants decreased along with increased salt stress (Babu et al., 2012). Salt stress during the inflorescence development increases flower abortion of tomato plants and causes a decrease in pollen number and viability (Ghanem et al., 2009). Moreover, salt stress at the flowering stage has a direct adverse effect on yield by reducing the number of tomato fruits (Zhang et al., 2017). Because the importance of the *NHX* family in regulating salt tolerance is well established, the roles of several *NHX* members in the tomato under salt stress have been reported (Baghour et al., 2019, 2023; Gálvez et al., 2012; Huertas et al., 2013; Maach et al., 2020, 2021; Olías et al., 2009). Gálvez et al. (2012) reported that *LeNHX1*, *−2*, *−3*, *−4* genes are generally induced by salt treatment in root, stem, and leaf tissues of salt-sensitive and salt-tolerant tomato species, and these isoforms are involved in Na^+ ion accumulation in the aerial parts of the plant. Overexpression of the *LeNHX2* (Huertas et al., 2013) and *LeNHX4* (Maach et al., 2020) genes in transgenic tomato plants has been reported to improve salinity tolerance. In the tomato, gene expression analyses of tomato *NHX* genes under salt stress in previous reports were mainly limited to root, leaf, or stem tissues, and there were also no reports focusing on determining the expression patterns of *NHX* genes in flower tissues under salt stress. Recently, Hussain et al. (2022) have reported the identification of seven *NHX* genes in the tomato using a genome-wide approach. Herein, we have discussed and reviewed the findings of Hussain et al. (2022) related to the *SlNHX* genes in the tomato.

In the present study, we identified members of the *NHX* gene family based on a comprehensive genome-wide approach using the current tomato genome and used bioinformatics tools to reveal phylogenetic relationships, synteny analysis, motif analysis, promoter analysis, protein–protein interaction (PPI), and gene structures.

Furthermore, the gene expression patterns of the identified *SlNHX* genes were also analyzed by RT-qPCR in the open flower tissues obtained at 0, 6, 12, and 24 h after the plants were treated with 240-mM NaCl shock.

2 | MATERIALS AND METHODS

2.1 | Identification and characterization of the *NHX* genes in tomato genome

To identify putative *NHX* genes in tomato, the Pfam ID (PF00999) number belonging to the *NHX* gene family was searched in the Phytozome database (Goodstein et al., 2012). In addition, keywords related to *NHX* genes, such as *sodium/hydrogen exchanger*, and Na^+/H^+ *antiporterI* were also searched in the Sol Genomics Network (Fernandez-Pozo et al., 2015). The presence of the *NHX* domain genes was also confirmed by the Hidden Markov Model (Cook et al., 2018). The peptide sequences of the hypothetical tomato *NHX* genes were aligned to the sequences of the *NHX* genes in Arabidopsis, and the percentage of identity between the hypothetical tomato *NHX* genes and the *AtNHX* genes was determined. The Arabidopsis Information Resource (TAIR) database was used to retrieve Arabidopsis NHX protein sequences (Berardini et al., 2015). The isoelectric point (pI) and molecular weight (MW) of the *SlNHX* genes were calculated with the ExPASy tool (Gasteiger et al., 2003). Intracellular localization of *SlNHX* genes was predicted with the Plant-mPLoc server (Chou & Shen, 2010). The peptide sequences of the *SlNHX* genes were screened with the TMHMM 2.0 web-based tool to confirm their transmembrane helix domains (Krogh et al., 2001).

2.2 | Multiple sequence alignment and phylogenetic analysis

The amino acid sequences of *NHX* genes of tomato and selected species (*A. thaliana*, *G. max*, *M. truncatula*, and *V. vinifera*) were used for multiple sequence alignment with the MUSCLE algorithm, and a phylogenetic tree was created using MEGA 11 software (Tamura et al., 2021). A thousand replicates were used to determine the bootstrap value. The phylogenetic tree was visualized via iTOL (Letunic & Bork, 2021).

2.3 | Chromosomal localization and synteny analysis

Sol Genomics Network database was used to visualize and to locate *SlNHX* genes on the chromosomes of tomato genome (Fernandez-Pozo et al., 2015). Phytozome and Ensembl databases were used to determine the genetic relationship of *S. lycopersicum* with *C. annuum*, *S. lycopersicum*, and *A. thaliana* (Cunningham et al., 2022). Fasta and GFF3 files were downloaded from related databases and analyzed with One Step MCScanX function in TBtools program (Wang et al., 2012). Analysis results were visualized via Dual Synteny Plot for MCScanX function in TBtools software (Chen et al., 2020).

2.4 | Conserved motif and gene structure analysis of *SlNHX* members

The Multiple Expectation Maximization for Motif Elicitation (MEME) Suite tool was used to identify conserved motifs in the amino acid sequences of the *SlNHX* gene family (Bailey et al., 2015). The TBtools software's Gene Structure View was used to show schematic representation of the *SlNHX* gene structure.

2.5 | Calculation of *Ka*/*Ks* and *cis*-regulatory element analysis

The *Ks* (synonymous) and *Ka* (non-synonymous) substitution of each duplicated gene pair were calculated using the Computational Biology Unit database (Siltberg & Liberles, 2002). The upstream 1500-bp region of the *SlNHX* genes was selected for analysis of *cis*-regulatory elements on the promoters and predicted using the PlantCARE tool (Lescot et al., 2002).

2.6 | Transcriptome profiling of *SlNHX* genes

The TomExpress RNA-Seq platform provided transcriptome data for the "Microtom" cultivar's roots, flowers, leaves, and flower buds tissues (Zouine et al., 2017). The results were displayed by using TBtools software after the data values were obtained as the normalized mean count per base of each *SlNHX* gene.

2.7 | Three-dimensional (3D) structure analysis and PPI of SlNHX proteins

The 3D structures of SlNHX proteins were created by using the I-TASSER tool (Yang & Zhang, 2015). The outputs of the I-TASSER modeling results were visualized by using the RCSB Protein Data Bank 3D Viewer (Berman et al., 2000). The prediction of the PPI network of SlNHX proteins was performed by using the STRING database (Jensen et al., 2009).

2.8 | Growth conditions of plant material and salt stress treatment

Tomato seeds (*S. lycopersicum* L., cv. Microtom) were sown on wet filter paper in plastic dishes and allowed to germinate in the dark at 25°C for 1 week. Germinated seeds were transferred to pots (125 × 73 mm) containing peat soil and perlite (3:1) in a plant growth

TABLE 1 The sequences of Forward (F) and Reverse (R) primers used in RT-qPCR reactions.

Accession number	Gene name	Primer sequence	Product size (bp)
Solyc01g067710	*SlNHX1*	F: GGCTTACCTATCTTACATGCTTGC R: AGCTCTCAGTCACATTATGCC	gDNA 244 cDNA 113
Solyc01g098190	*SlNHX2*	F: TCCTCTTCCTCTATGTGGGCA R: AAACAAAAGCAGCTCTCCCCA	gDNA 314 cDNA 135
Solyc10g006080	*SlNHX3*	F: CTCAGTGGGATTTTGACCGTC R: CAATGTCCAACGCATCCATCC	gDNA 522 cDNA 169
Solyc06g008820	*SlNHX4*	F: ACTGATCGTGAAGTTGCTCTC R: TGCCAGGTATAGTGTGACATG	gDNA 209 cDNA 128
Solyc04g056600	*SlNHX6*	F: TCTTGTACGACCTCCACACC R: GGACTGACTGCAAAGCAAGG	gDNA 192 cDNA 107
Solyc01g005020	*SlNHX7*	F: CCTGGCGTGCTTATTTCCAC R: CCCAATTTCTTGCTGGCACC	gDNA 242 cDNA 167
Solyc04g018100	*SlNHX8*	F: CTTTTGCTTGCTGGACCTGG R: ACAGCCACAGGATCAGTAGC	gDNA 209 cDNA 140
Solyc07g025390	*EXPRESSED* (housekeeping)	F: GCTAAGAACGCTGGACCTAATG R: TGGGTGTGCCTTTCTGAATG	gDNA 291 cDNA 183

chamber with 25 ± .5°C temperature, 65 ± 5% humidity, and 18/6 h (day/night) photoperiod (350 µmol m^{-2} s^{-1}). The commercial liquid fertilizer (Black Diamond) was applied with irrigation as needed while no pesticide was used. Because the toxic effects of salt were not observed in the open flower tissues in our preliminary experiments using different concentrations of NaCl (60, 120, and 180 mM), the 240-mM NaCl salt shock was applied to the plants as at the flowering stage. Furthermore, previous reports support the suitability of high salt concentration in the tomato Microtom cultivar (Bacha et al., 2017). Open flower tissues were collected from three biological replicates at 0 (control), 6, 12, and 24 h after salt shock treatment and were immediately stored at −80°C until total RNA extraction.

2.9 | Total RNA isolation and cDNA synthesis

Total RNA was isolated from open flower tissues by using the GF-1 Total RNA Extraction Kit, followed by DNase treatment to eliminate genomic DNA contamination. The quality of the isolated RNA was checked with both gel electrophoresis and a NanoDrop One (Thermo Scientific™ NanoDrop™ One Microvolume UV–Vis Spectrophotometers) instrument. The first-strand cDNA was synthesized by using RevertAid First Strand cDNA Synthesis Kit (Thermo Scientific™).

2.10 | Real time-quantitative PCR (RT-qPCR)

RT-qPCR reactions were carried out using the Ampliqon RealQ Plus SYBR Green/ROX Master Mix Kit. Gene-specific forward and reverse primers for members of *SlNHX* gene family were designed using MacVector v18.2 software (MacVector Inc., Cary, NC, USA) (Table 1). The *EXPRESSED* gene was used as housekeeping for normalization in RT-qPCR analyses (Choi et al., 2018). The RT-qPCR conditions: initial denaturation at 95°C for 8 min, 40 cycles of 95°C denaturation for 15 s, 55°C annealing for 30 s, and 72°C extension for 30 s. Three biological replicates were used for each sample. The relative expression levels of the *SlNHX* genes were calculated by the $2^{-\Delta\Delta Ct}$ method (Livak & Schmittgen, 2001).

2.11 | Statistical analysis

GraphPad Prism 9.3 software (GraphPad Software Inc., San Diego, CA, USA) was employed to perform statistical analysis. The data were statistically analyzed using one-way analysis of variance (ANOVA), and the difference was considered significant when the *p value* was less than .05.

3 | RESULTS

3.1 | Identification of *SlNHX* genes

The amino acid sequences of *AtNHXs* were used in the alignments to identify the *NHX* gene family in the tomato genome. The results revealed seven *SlNHX* genes encoding the *NHX* in the tomato genome (Table 2), namely, *SlNHX1* (Solyc01g067710), *SlNHX2* (Solyc01g098190), *SlNHX3* (Solyc10g006080), *SlNHX4* (Solyc06g008820), *SlNHX6* (Solyc04g056600), *SlNHX7* (Solyc01g005020), and *SlNHX8* (Solyc04g018100).

Sequence analyses revealed that genomic sequences of *SlNHX* genes ranged from 4232 bp (*SlNHX3*) to 15,997 bp (*SlNHX6*), the number of exons in the coding sequence (CDS) ranged from 14 to 23, and the total length of CDS ranged from 1578 bp (*SlNHX3*) to 3456 bp (*SlNHX7*) (Table 2). The size of ORF ranged from 526 aa (*SlNHX3*) to 1152 aa (*SlNHX7*) (Table 2). In addition, the size of SlNHX

TABLE 2 Some characteristics of tomato *SlNHX* genes.

Gene name	Accession number	Genomic sequence (bp)	CDS (bp)	ORF (aa)	TM	Ch	NHX class	Subcellular localization	MW (kDa)	pI	Identity with NHX protein of Arabidopsis (%)
SlNHX1	Solyc01g067710	4956	1614	538	10	1	I	Vacuole	59.4	8.55	72.5
SlNHX2	Solyc01g098190	5857	1611	537	10	1	I	Vacuole	58.7	7.24	75.5
SlNHX3	Solyc10g006080	4232	1578	526	11	10	I	Vacuole	59.1	8.48	69.9
SlNHX4	Solyc06g008820	7602	1605	535	10	6	I	Vacuole	59.0	6.60	63.1
SlNHX6	Solyc04g056600	15,997	1596	532	12	4	II	Vacuole	58.5	5.42	81.6
SlNHX7	Solyc01g005020	13,405	3456	1152	12	1	III	CM	127.5	5.89	64.4
SlNHX8	Solyc04g018100	15,127	2952	983	10	4	III	CM-vacuole	108.2	5.75	49.8

Abbreviations: CDS, coding sequences; Chr, chromosomal location; CM, cell membrane; MW: molecular weight; ORF: open reading frame; pI: isoelectric point; TM: transmembrane domain.

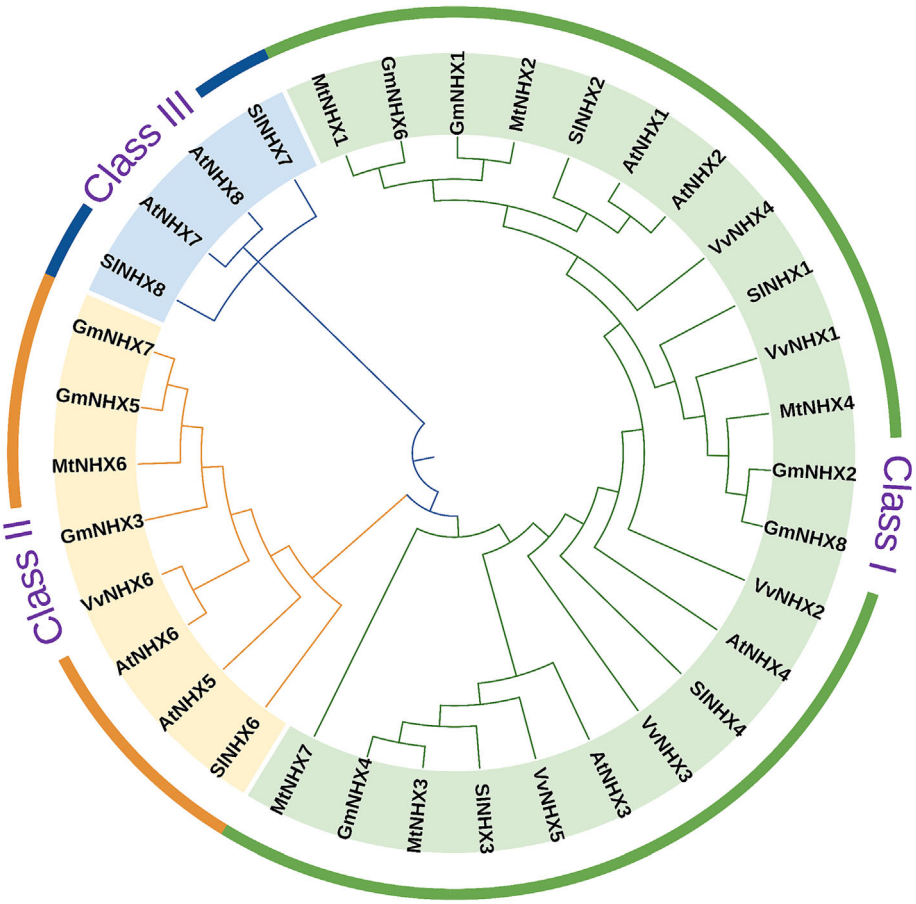

FIGURE 1 Phylogenetic relationships among Na^+/H^+ *antiporter* (NHX) proteins of tomato and selected species, *Solanum lycopersicum* (Sl), *Arabidopsis thaliana* (At), *Medicago truncatula* (Mt), *Glycine max* (Gm), and *Vitis vinifera* (Vv).

proteins ranged from 58.5 (kDa, SlNHX6) to 127.5 (kDa, SlNHX7), whereas isoelectric points (pI) varied from 5.42 (SlNHX6) to 8.55 (SlNHX1) (Table 2). SlNHX proteins had transmembrane domains ranging from 10 to 12 (Table 2). The amino acid sequences of the *SlNHX* genes were aligned with the amino acid sequences of the *AtNHX* genes, and the identity of the genes with the *AtNHX* genes was determined. The highest identity matrix score (81.6%) was determined between *SlNHX6* and *AtNHX6* genes, whereas the lowest (49.8%) was between *SlNHX8* and *ATNHX8* genes (Table 2).

3.2 | Phylogenetic analysis

To determine the evolutionary relationships of NHX proteins with some of other plant species, SlNHXs were compared with *A. thaliana* (At, eight sequences), *G. max* (Gm, eight sequences), *M. truncatula* (Mt, six sequences), and *V. vinifera* (Vv, six sequences). These plant species were chosen due to their status as model plants and their representation in several plant families allowing the investigation of the evolution and diversity of *NHX* genes. A total of five species were used for

the analysis, as the results of the preliminary phylogenetic analysis showed that including more plant species in the phylogenetic analysis led to reduced interpretability. Phylogenetic analysis revealed that 35 SlNHX proteins were divided into three classes based on their predicted subcellular localization, indicated by different colors using iTOL program (Figure 1). *SlNHX1*, *−2*, *−3*, and *−4* were localized on the vacuole membranes (Vac class/Class I); *SlNHX6* was localized on the endosomal region (Endo class/Class II); and *SlNHX7* and *−8* were localized on the PM (PM class/Class III) (Figure 1).

3.3 | Chromosomal localization, *Ka/Ks*, and synteny analysis

Location information of *SlNHX* genes on the chromosomes was obtained from the tomato genome. Seven putative *SlNHX* genes were scattered on 4 chromosomes. *SlNHX3* gene was located on chromosome 10; genes *SlNHX6* and *SlNHX8* were located on chromosome number 4; *SlNHX1*, *−2*, and *−7* genes were located on chromosome 1, and *SlNHX4* gene was located on chromosome 6 (Figure 2). There were no *SlNHX* genes on chromosomes 2, 3, 5, 7, 8, 9, 11, and 12.

The formula $T = (Ks/2\lambda) \times 10^{-6}$ million years ago was used to estimate the date of duplication events ($\lambda = 1.5 \times 10^{-8}$) (Blanc & Wolfe, 2004; Madrid-Espinoza et al., 2019). According to the *Ka/Ks* ratio, the selection type is divided into three different groups as purifying (*Ka/Ks* < 1), neutral (*Ka/Ks* = 1), and positive selection (*Ka/Ks* > 1) (Table 3) (Lynch & Conery, 2000). The term "tandem duplication" refers to the presence of two or more genes on the same chromosome, whereas the term "segmental duplication" refers to the presence of genes on different chromosomes (Table 3) (Akram et al., 2020).

To better understand the evolutionary relationships of the *SlNHX* genes, comparative syntenic schemes were constructed between *S. lycopersicum*, *C. annuum*, and *A. thaliana* genomes. The *SlNHX1*, *SlNHX2*, *SlNHX3*, and *SlNHX7* genes showed collinear relationships with *A. thaliana* and *C. annuum* (Figure 3). *SlNHX4*, *SlNHX6*, and *SlNHX8* genes did not show a synteny with the genomes compared (Figure 3).

3.4 | Gene structure and conserved motif analysis

The exons and introns of *SlNHXs* genes were analyzed by using TBtools. Vac class *SlNHX1*, *−2*, *−3*, and *−4* genes provided 14 exons and 13 introns (Figure 4). Endo class *SlNHX6* had 22 exons and 21 introns, whereas PM class *SlNHX7* and *SlNHX8* genes showed 23 exons and 22 introns and 22 exons and 21 introns, respectively (Figure 4). Among the *SlNHXs* genes, *SlNHX6* had the largest genomic sequence length at 15997 bp, whereas *SlNHX3* had the shortest with

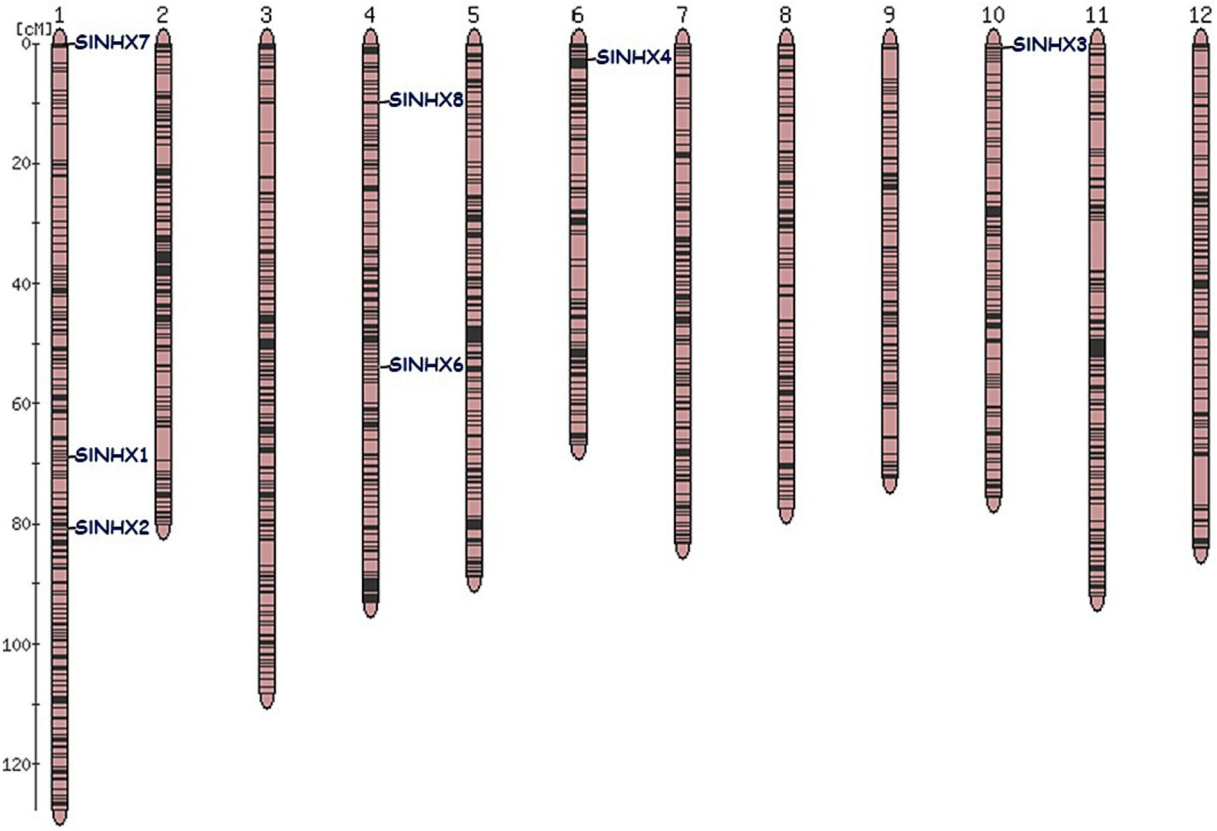

FIGURE 2 The chromosomal distribution of *SlNHX* gene family members in the tomato genome.

TABLE 3 *Ka*/*Ks* ratio, duplication, selection types, and divergence time of *SlNHX* genes.

Gene pairs	*Ka*	*Ks*	*Ka/Ks*	Duplicated type	Selection type	Time (million year ago)
SlNHX7-SlNHX8	.183	.402	.456	Segmental	Purify	3.011
SlNHX3-SlNHX4	.132	.417	.316	Segmental	Purify	3.126
SlNHX1-SlNHX2	.068	.407	.166	Tandem	Purify	3.054

Abbreviations: *Ka*, the number of nonsynonymous substitutions per non-synonymous site; *Ks*, the number of synonymous substitutions per synonymous site.

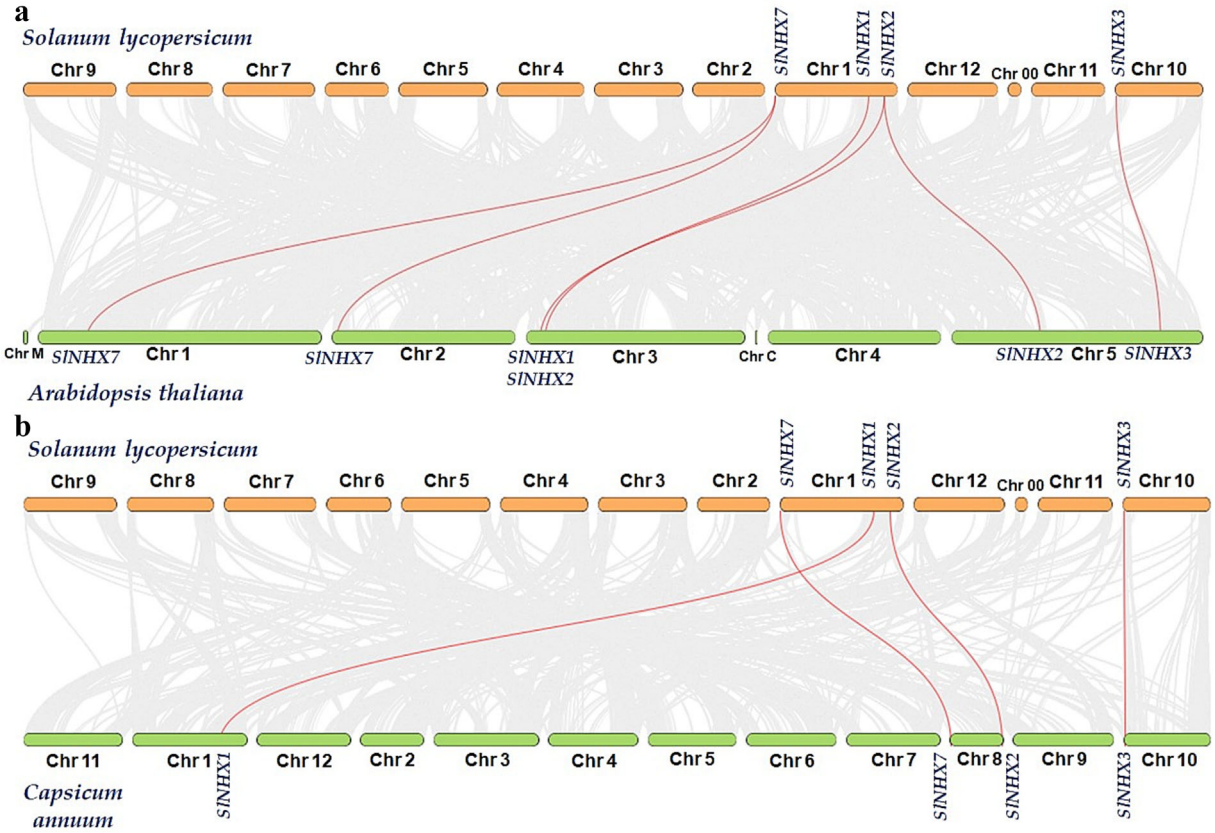

FIGURE 3 Comparative synteny analysis of Na^+/H^+ *antiporter* (*NHX*) genes in *Solanum lycopersicum*, *Arabidopsis thaliana*, and *Capsicum annuum* genomes. (a) Syntenic relationship among *SlNHX* genes in *S. lycopersicum* and *A. thaliana*. (b) Syntenic relationship among *SlNHX* genes in *S. lycopersicum* and *C. annuum*. The gray lines in the background represent the synteny pairs of the whole genome, whereas the red lines indicate the synteny of *SlNHX* gene pairs and their corresponding positions on each chromosome.

4232 bp. The *NHX* domain (PF00999) was also confirmed by using the Hidden Markov Model (HMM).

Parameter settings related to motif analysis: the maximum number of motifs was 16, and the optimum aa width was set to 6–50 in length. The MEME tool was used to investigate the conserved motifs of *SlNHX* genes, and the conserved motifs were determined in different colors (Figure 5a). Analysis results revealed that there were 10 conserved motifs in *SlNHX* family members, and these conserved motifs ranged from 21 to 50 amino acids in length (Figure 5a). Whereas motif 1 was found in all members of *SlNHX*, motifs 2, −3, −4, −5, −6, −7, and −9 were found in the members of *SlNHX1*, −*2*, −*3*, and −*4* (Figure 5a). Motif 10 was also found in members of *SlNHX6*, −*7*, and −*8*, whereas Motif 8 was found in all members except in *SlNHX7* and *SlNHX8* genes (Figure 5a). The amiloride binding site [FFIYLLPPI], which is a characteristic feature of NHX proteins, was fully conserved in *SlNHX1*, −*2*, and−*3* genes, whereas it mostly retained in *SlNHX4* and *SlNHX6* genes. The amiloride binding site was absent in *SlNHX7* and *SlNHX8* genes (Figure 5b).

3.5 | Analysis of *cis*-regulatory elements of *SlNHX* genes

Analysis of *cis*-regulatory elements in the 1500 bp upstream promoter region of *SlNHX* genes was performed with the PlantCare tool (Figure 6). The results indicated that the *SlNHX* genes family contained

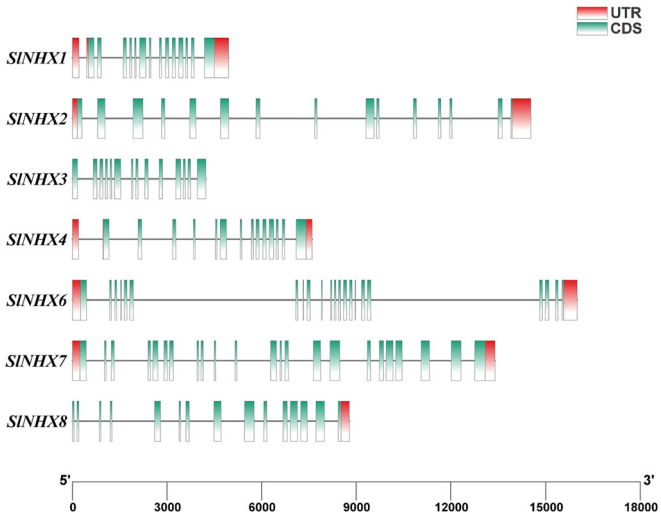

FIGURE 4 The gene structure of Na^+/H^+ *antiporter* (*NHX*) family member in the tomato. CDS, coding sequence; UTR, untranslated region. The scale is given as bp.

a total of 502 *cis*-regulatory elements, and they were classified in a total of 32 types, which were mainly related to light-responsible elements, development-related elements, hormone-responsible elements, promoter-related elements, site-binding-related elements, and environmental stress-related elements (Figure 6). Of those, the CAAT and TATA-boxes of promotor-related elements were too common and were included an average of 12.14 and 55.71 times, respectively, in the defined promotor regions of all *SlNHX* genes and did not provide a unique pattern as *cis*-regulatory elements, respectively (data not shown). On the other hand, the light-responsible elements included 3-AF1 binding site, AT1-motif, ATCC-motif, ATC-motif, ACE, AE-box, Box 4, chs-CMA1a, GA-motif, GATA-motif, G-Box, GT1-motif, G-box, I-box, LAMP-element, MRE, and TCT motif (Figure 6a). Development-related elements included O2-site, CAT-box, and circadian motifs (Figure 6a,b). Hormone-responsible elements included ABRE, TGACG-motif, GARE-motif, TATC-box, and CGTCA-motif (Figure 6a,b). Site-binding-related elements included AT-rich element, Box, and Unnamed_1 (60K protein binding site). Environmental stress-related elements included LTR, MBS, TC-rich repeats, and ARE (Figure 6a,b). The ABRE (ABA, the abscisic acid), TGACG-motif (MeJA), GARE-motif (GB, Gibberallin), TATC-box (MeJA), and CGTCA-motif (MeJA) were determined to be hormone-related *cis*-acting regulatory elements (data not shown). Of those elements, MeJA-related *cis*-acting regulatory elements (twice of TGACG-motif and CGTCA-motif and single TATC-box) were located on the *SlNHX6* (data not shown).

3.6 | PPI prediction

The PPI network was built by the STRING database using the K-means Clustering algorithm (network is grouped to a predefined number of clusters) to further investigate the probable role of SlNHXs during possible interactions with other proteins. Based on the clustering analysis, the network is divided into three clusters based on the clustering analysis. Cluster 1 (red Bubble) contains the proteins CBL10, SlNHX7, CIPK, and Solyc06g051970; Cluster 2 (Green Bubble) contains the proteins SlNHX1, SlNHX2, SlNHX4, SlNHX6, Solyc07g014680, and Solyc08g065360; and Cluster 3 (Blue Bubble) contains the proteins SlNHX3 and SlNHX8. The analysis results showed that the proteins SlNHX7 and SlNHX8 hypothetically interacted with Calcineurin B-like (CBL) and CBL-interacting protein kinases (CIPK) (Figure 7). Solyc07g014680 (Putative High-affinity K^+ transporter 1) interacted with all proteins in the network. In addition, Solyc06g051970 (Calcineurin B-Like Protein 4) also interacted with all proteins apart from CBL10 (Calcineurin B-like Protein 10) in the tomato genome network.

3.7 | Three-dimensional (3D) structure prediction of SlNHX proteins

The 3D model structures of SlNHX proteins were obtained by using the I-TASSER tool and visualized using the PDB 3D Viewer (Figure 8). The C-score was used to estimate the confidence of the models created in the analysis for SlNHX proteins (Roy et al., 2010). The C-score is a confidence score for estimating the quality of predicted models by I-TASSER (Yang et al., 2013). The C-score generally varies in the range of [−5, 2], and the higher the score, the higher the reliability of the model (Yang et al., 2013). TM-score was proposed to scale for measuring the structural similarity between two structures, and it ranges from 0 to 1 and a value of 1 indicating a perfect match between the two constructs (Zhang, 2008). The root-mean-square deviation (RMSD) varies between 0 and 30 angstrom (Å) (Roy et al., 2010). The analysis results revealed that C-scores of the SlNHX proteins ranged from −1.33 to .35 (Table 4). The modeling estimate of the SlNHX4 protein gave the highest C-score at .35, whereas the SlNHX7 and SlNHX8 proteins had the lowest C-score at 1.33 (Table 4). The length of the *NHX* domain in SlNHX proteins ranged from 418 (SlNHX3) to 404 (SlNHX6) amino acids (Table 4).

3.8 | RNA-Seq gene expression profiles of *SlNHX* genes

The high-throughput gene expression data analysis was retrieved from the TomExpress database, and the Microtom cultivar was selected to determine the expression levels of tissue-specific *SlNHX* genes. Seven *SlNHX* genes and types of tissues including root, flower, leaf, and flower buds were selected to generate the heatmap using TBtools (Figure 9). According to expression patterns, all *SlNHX* genes except the *SlNHX1* gene were expressed in all tissues (Figure 9). The *SlNHX2* gene was expressed at high levels in all tissues, whereas the *SlNHX1* gene showed the lowest expression levels (Figure 9). In addition, the heatmap revealed that the *SlNHX2* and *SlNHX6* genes were highly expressed in flower tissue while the *SlNHX3* and *SlNHX*1 genes showed the lowest expression levels.

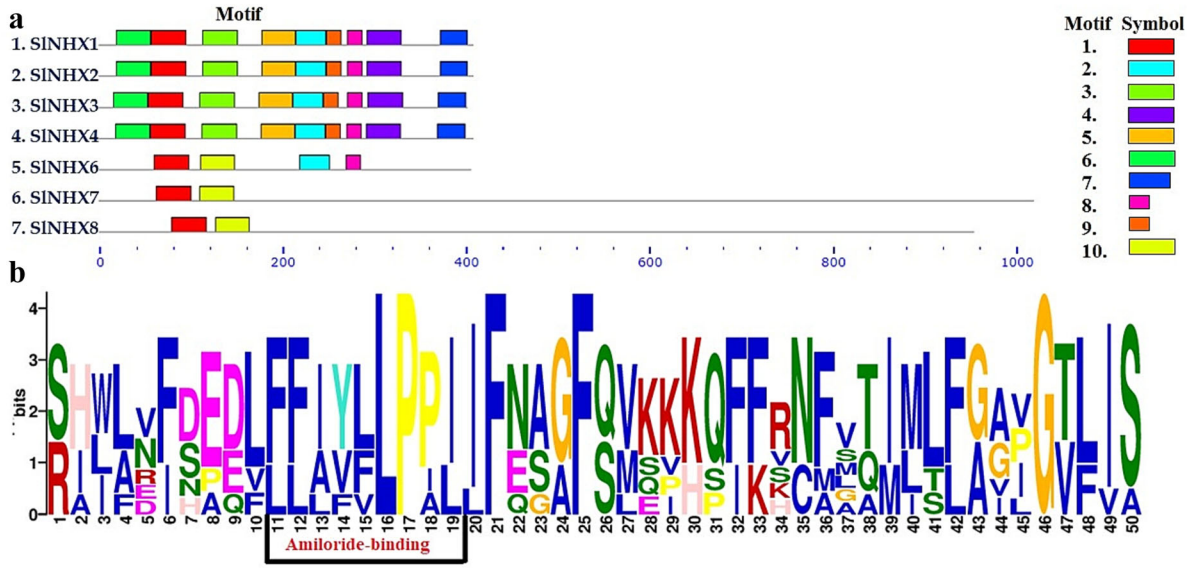

FIGURE 5 Conserved motif analysis of *SlNHXs* genes. (a) Conserved motifs of *SlNHXs* genes, (b) motif 1 was found in all *SlNHX* genes, and it had an amiloride binding site [FFIYLLPPI]. The scale showing the sequence length of the proteins was shown below (up to 1000 aa).

3.9 | Expression profiles of the *SlNHX* genes under salt shock

Relative expression levels of *SlNHX* genes were determined in the open flower tissues collected at the given time intervals (0th, 6th, 12th, 24th h) after 240-mM NaCl shock was applied. The expression of *SlNHX* genes was normalized with the *EXPRESSED* (Solyc07g025390) gene (Figure 10). The RT-qPCR data indicated that salt shock significantly changed the relative expression levels of all *SlNHX* genes in all given time intervals with some exceptions (Figure 10). For instance, salt shock significantly changed the relative expression levels of *SlNHX3*, *SlNHX4*, *SlNHX7*, and *SlNHX8* genes in all given time intervals compared with control, whereas significant levels of the relative expression levels of *SlNHX1*, *SlNHX2* and *SlNHX6* genes were various based on given time intervals (Figure 10). An increased relative expression level of the *SlNHX6* gene was delayed until the 12th hour of salt shock, whereas *SlNHX1* and *SlNHX2* genes showed early significant upregulations after 6 h of salt shock (Figure 10). Among *SlNHX* gene family members, *SlNHX1*, *SlNHX2*, and *SlNHX8* genes were substantially upregulated in the open flower tissues at the 6th hour of salt shock, whereas significant downregulations were determined for the relative gene expressions levels of *SlNHX3* and *SlNHX7* genes at the same time interval (Figure 10). In contrast to the other *SlNHX* gene family members, the relative expression levels of *SlNHX6*, *SlNHX7*, and *SlNHX8* genes were the highest at the 24th hour of salt shock (Figure 10).

4 | DISCUSSION

Abiotic environmental factors such as salinity directly affect plant growth and development and cause severe agricultural yield losses (Van Zelm et al., 2020). The *NHX* genes are significant in maintaining Na^+ ion homeostasis in plant tissues, and many reports have revealed that these genes provide salt tolerance to plants (Li et al., 2017). The availability of high-quality de novo genome assemblies and annotations (ITAG4.0) for the tomato reference genome (SL4.0) has opened up new opportunities for precision genome-wide studies in the tomato (Hosmani et al., 2019). In this study, a total of seven *NHX* genes were identified in the tomato, but the orthologue of the *NHX5* gene was not identified in the tomato genome. Although the Solyc04g056600 accession showed identity to both *AtNHX5* (80.6%) and *AtNHX6* (81.6%) genes of Arabidopsis at the amino acid levels, it was defined as the *SlNHX6* gene in the present study because of its higher identity score (%81.6) and no presence of *AtNHX5* gene orthology in the current tomato genome (Table 2). A similar case was also reported in the *M. truncatula* genome (Sandhu et al., 2018), suggesting that the *NHX5* gene does not share a common ancestor with *S. lycopersicum* and *M. truncatula* genomes by speciation although orthologous genes retained the same function in the course of evolution. Single knockout mutants of the *nhx5* and *nhx6* genes in *A. thaliana* have shown unaltered salt sensitivity, whereas double knockout mutants of the *nhx5* and *nhx6* genes have exhibited greater salt sensitivity than the wild-type plant (Bassil et al., 2011). This suggests that the absence of the *AtNHX5* gene orthologue in the tomato genome may not have a significant effect on the development of salt tolerance in the tomato (Sandhu et al., 2018). Although Hussain et al. (2022) previously reported seven *SlNHXs* in the tomato genome as in the present study, the genes identified are completely different from each other. Interestingly, the *Solyc00g021510* gene, which Hussain et al. (2022) identified as *SlNHX1*, is not present in the current tomato reference genome (SL4.0). The orthologue of *AtSOS1* in the tomato genome was identified as *SlSOS1* (CAG30524.1) by Olías et al. (2009), and this gene is identical to the *SlNHX7/SlSOS1* (Solyc01g005020) gene identified in the present study.

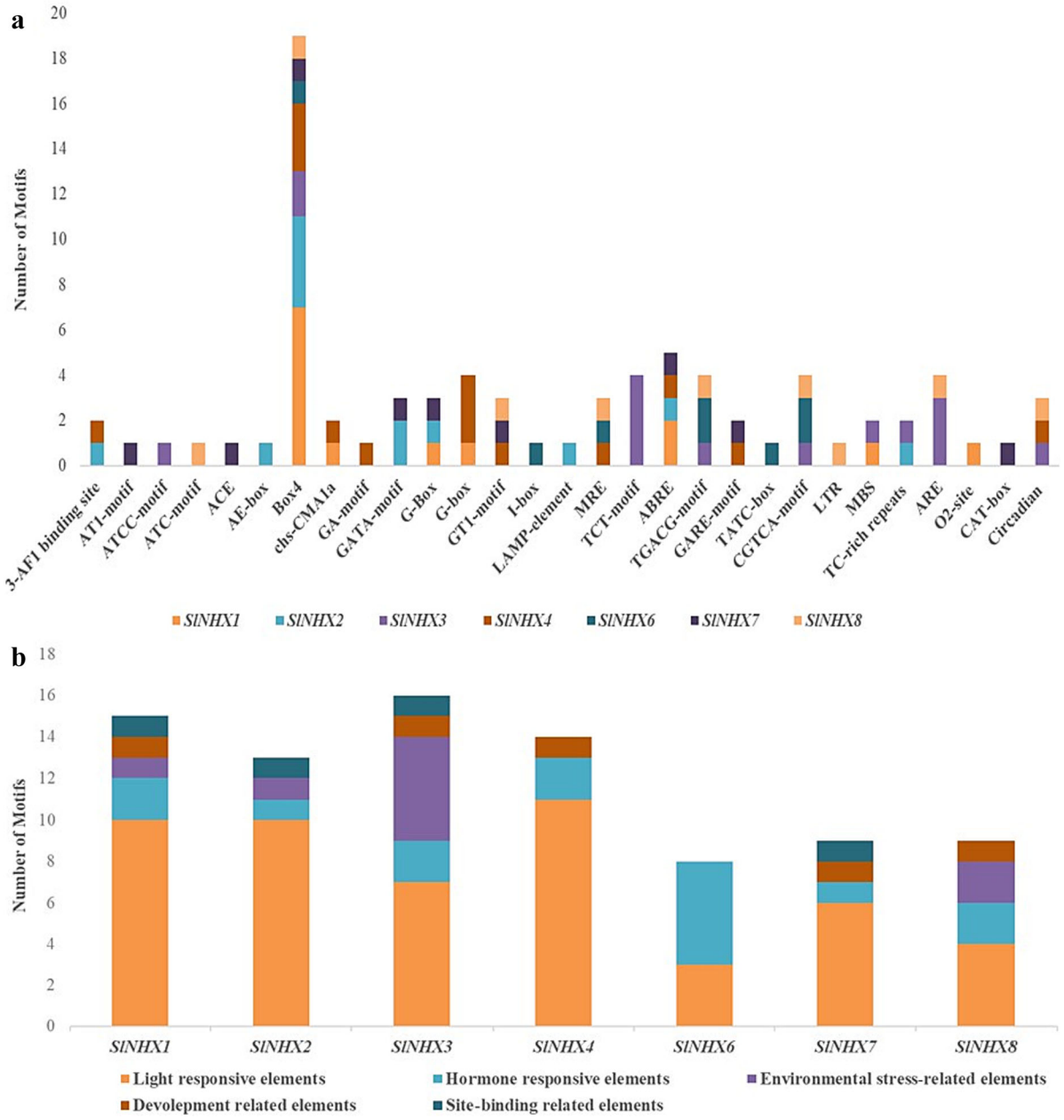

FIGURE 6 *Cis*-regulatory elements in the 1500 bp upstream promoter region of *SlNHX* genes. (a) Predicted *cis*-acting elements in the promoters of *SlNHX* genes, (b) different colored histograms represent categorical *cis*-acting elements in *SlNHX* genes.

Phylogenetic analysis revealed that 23 out of 35 NHX proteins and the majority of SlNHX (SlNHX1, −2, −3, and −4) proteins bind to vacuolar membrane, and the PM and Endo classes contained 6 and 8 proteins, respectively (Figure 1). A similar pattern of cluster was also reported for other plant species including cotton (Fu et al., 2020), sugar beet (Wu et al., 2019), and honeysuckle (Huang et al., 2022). *LeNHX2* was previously located in the Endo class (Class II), which includes *AtNHX5* and *AtNHX6* (Gálvez et al., 2012; Huertas et al., 2013; Rodríguez-Rosales et al., 2008; Venema et al., 2003), whereas the *SlNHX2* member identified in this study was located in the Vac class (Class I), which includes *AtNHX1*, *AtNHX2*, *AtNHX3*, and *AtNHX4* (Figure 1). Similarly, *MtNHX2* in the *M. truncatula* genome (Sandhu et al., 2018), *BvNHX2* in the *B. vulgaris* genome (Wu et al., 2019), and *PgNHX2* in the *P. granatum* genome were also localized in Vac class (Dong et al., 2021). As previously reported for other plant species (Dong et al., 2021; Fu et al., 2020; Huang et al., 2022; Sandhu et al., 2018; Wu et al., 2019), the *SlNHX* gene family was divided into three subgroups (Figure 1) although Hussain et al. (2022) provided two subgroups for the same gene family designated as N1 and N2. Moreover, Hussain et al. (2022) included the *SlNHX1* and *SlNHX2* genes in the same subgroups as *AtNHX7* and *AtNHX8*, which belong to the PM class.

The transmembrane domain numbers and amiloride binding domains of SlNHX proteins were similar to most *NHX* family members

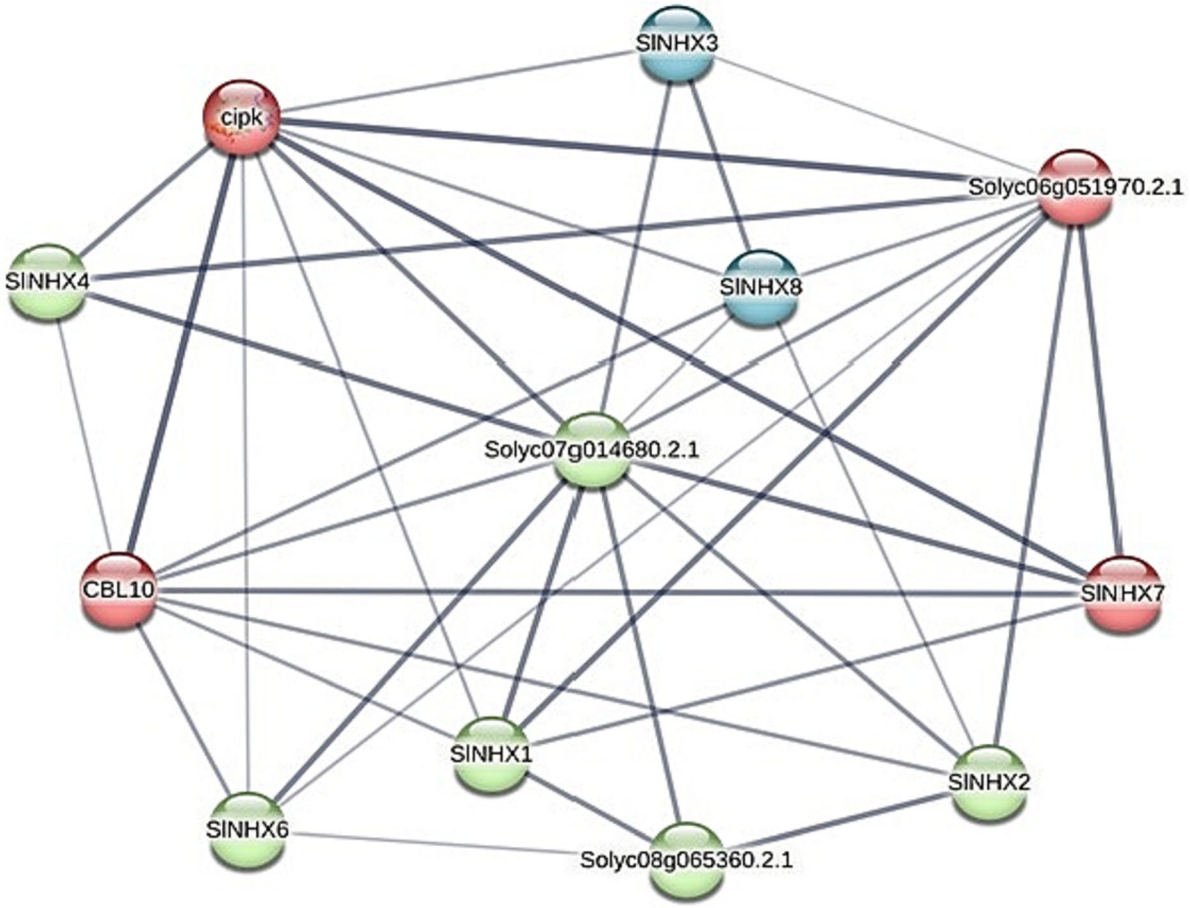

FIGURE 7 Protein–protein interaction (PPI) network of SlNHXs. The lines (gray) represent the shared physical complex, and as the thickness of these lines increases, the confidence of interaction also increases. Each node represents all the proteins produced by a single, protein-coding gene locus. Empty nodes represent proteins with an unknown three-dimensional model. Filled nodes show that a three-dimensional model is known or predicted.

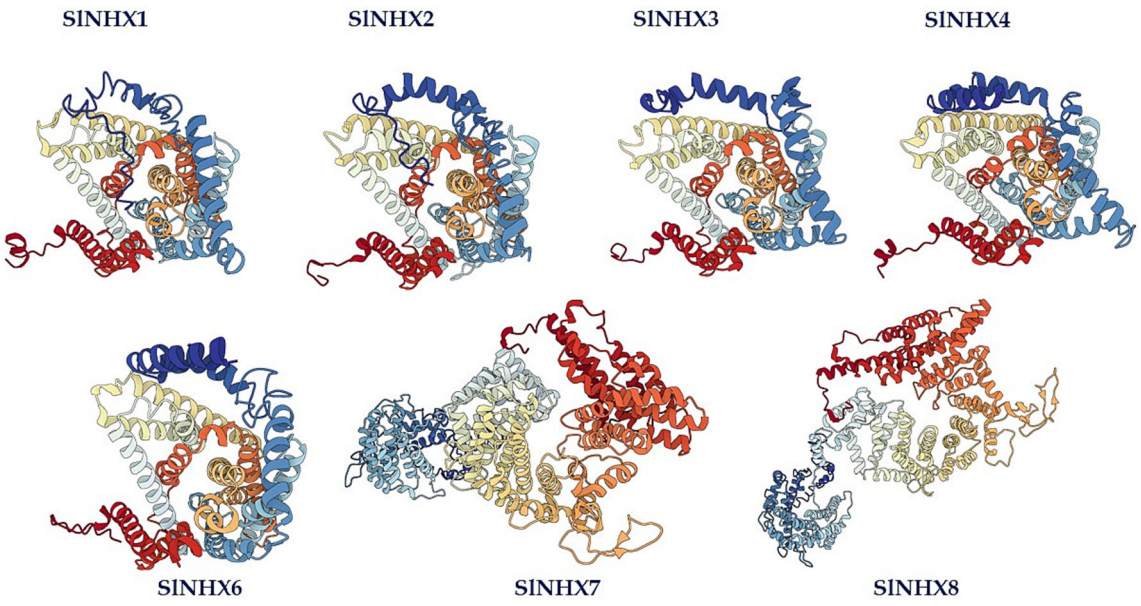

FIGURE 8 Three-dimensional structure prediction of seven SlNHX proteins.

TABLE 4 Quantitative outputs of I-TASSER modeling for SlNHX proteins and sequence location information of the *Na+/H+ antiporter* domain and amiloride binding sites.

Protein	C-score	TM-score	RMSD (Å)	Peptide sequence	Na^+/H^+ *antiporter* domain (start to end)	Amiloride binding site (start to end)
SlNHX1	−.23	.68 ± .12	8.0 ± 4.4	538	29–443	85–93
SlNHX2	−.16	.69 ± .12	7.8 ± 4.4	537	29–442	85–93
SlNHX3	.04	.72 ± .11	7.3 ± 4.2	526	27–444	81–89
SlNHX4	.35	.76 ± .10	6.7 ± 4.0	535	27–442	84–92
SlNHX6	−.16	.69 ± .12	7.8 ± 4.4	532	34–437	89–97
SlNHX7	−1.33	.55 ± .15	12.5 ± 4.3	1,152	29–441	-
SlNHX8	−1.33	.55 ± .15	12.5 ± 4.3	983	55–462	-

Abbreviation: RMSD, root-mean-square deviation.

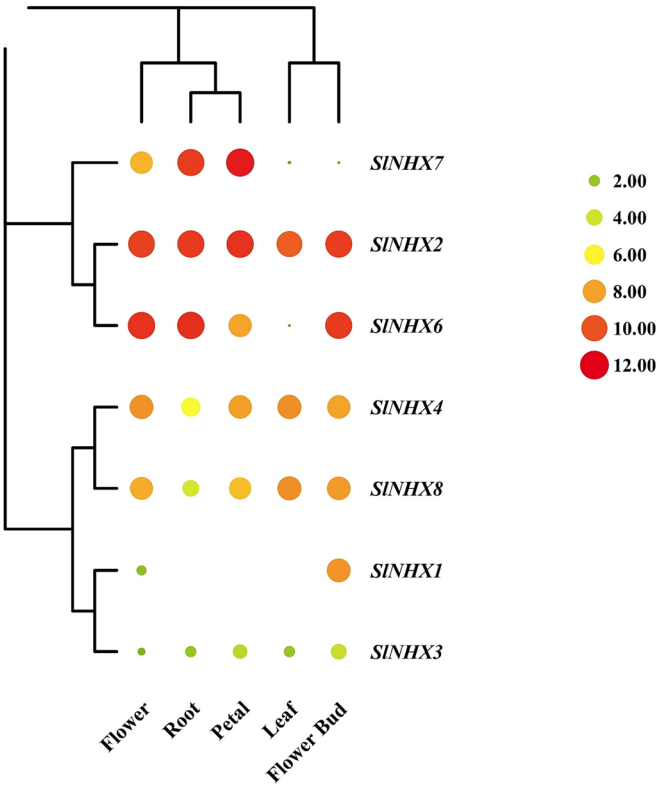

FIGURE 9 RNA-Seq gene expression profiles of *SlNHX* genes in different tissues.

of other species reported in the literature (Chen et al., 2015; Dong et al., 2021; Fu et al., 2020; Huang et al., 2022; Tian et al., 2017; Wu et al., 2019). The amiloride binding domain is either completely or highly conserved in plant species such as *A. thaliana*, *M. truncatula*, *P. granatum*, and *P. trichocarpa* (Aharon et al., 2003; Dong et al., 2021). The results of this study showed that the amiloride binding domain is fully conserved in *SlNHX1–3* genes and highly conserved in the *SlNHX4* and *SlNHX6* genes, whereas this site is absent in *SlNHX7* and *SlNHX8* genes (Figure 5b), which was in agreement with a previous report (Sandhu et al., 2018). In contrast, the *SlNHX1* and *SlNHX2* genes identified by Hussain et al. (2022) do not have an amiloride binding domain, whereas, interestingly, *SlNHX7* has this domain. Unlike the results reported by Hussain et al. (2022), the results of the present study were able to fully explore the amiloride binding domains of SlNHX proteins.

The results of synteny analysis revealed that there are four homologous pairs between tomato and pepper and four homologous pairs between tomato and Arabidopsis (Figure 3). These results indicated that *SlNHX* genes are phylogenetically related to *NHX* genes of different plant species. Generally, the *Ka/Ks* ratio of *SlNHX* genes was lower than 1, indicating a selection pressure on protein coding sequences during the evolution (Table 3) (Hanada et al., 2007). Similar low *Ka/Ks* ratios were also reported for honeysuckle (Huang et al., 2022), radish (Wang et al., 2020) and cotton (Fu et al., 2020). The protein–protein network of SlNHXs revealed that SlNHX7 and SlNHX8 interact physically with the CBL and CIPK proteins, unlike the other SlNHX proteins (Figure 6). It was previously shown that the *NHX7* gene, which provides tolerance by transporting Na^+ ions under salt stress in plants, was activated as a result of the interaction between CBL and CIPK proteins (Weinl & Kudla, 2009). Comparably, the interaction of CIPK and CBL proteins with NHX7 was also predicted in plant species such as poplar, sugar beet, and pomegranate (Dong et al., 2021; Tian et al., 2017; Wu et al., 2019). These results revealed that *SlNHX7* and *SlNHX8* genes could play a more important role than the other *SlNHX* genes in responses to salt stress in the tomato genome.

The results of RT-qPCR revealed that *SlNHX6* and *SlNHX8* genes showed significant and elevated upregulation by salt stress in the open flower tissues as the stress expanded to 24 h, and an early salt stress response (at 6th h) was provided by the *SlNHX1* and *SlNHX2* genes (Figure 10). These results were comparable with RNA-Seq gene expression profiles of *SlNHX* genes determined in different tissues (Figure 9). A similar gene expression pattern of *SlNHXs* could also be possible in other tissues at various developmental stages of tomato (Figure 10). In addition, presence of the higher number of MeJA-related *cis*-acting regulatory elements on the promotor regions of *SlNHX6* (TATC-box, TGACG, CGTCA) and *SlNHX8* (TGACG, CGTCA), compared with the other promotors of *SlNHXs*, may also be attributed to the significant and elevated upregulation of these genes (Figure 10). These findings suggested that *SlNHX* genes in *S. lycopersicum* might provide

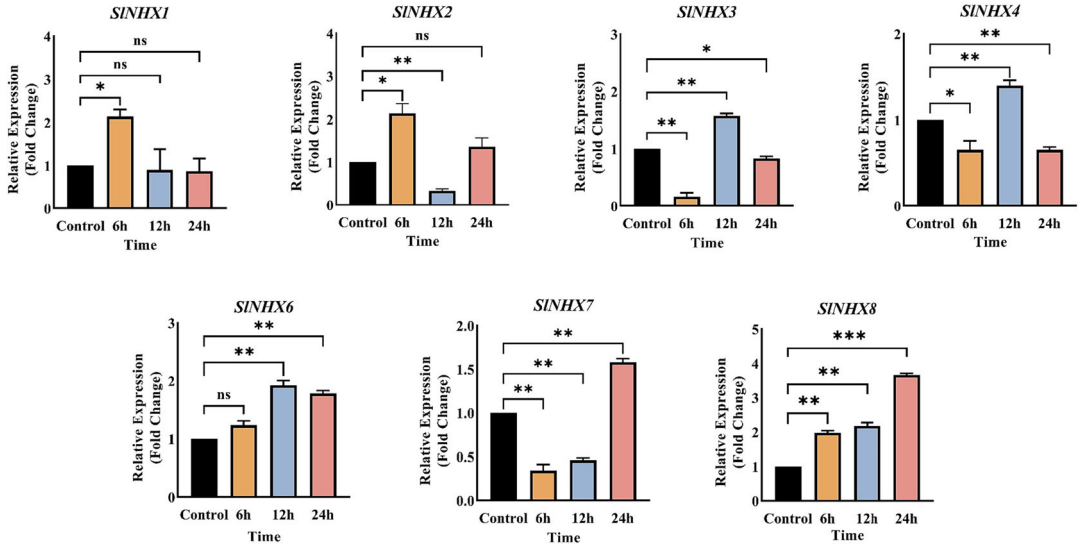

FIGURE 10 Relative gene expression profiles of *SlNHX* gene family members at different time intervals under 240-mM NaCl shock. Error bars show the standard error of three biological replicates mean ($n = 3$) (ns: no significant; $^{*}p < .05$; $^{**}p < .01$; $^{***}p < .001$).

orchestrated and time-dependent responses based on the duration and severity of salt stress (Figure 10). In the *LeNHX* isoforms induced by salt treatment, the greatest induction was in the *LeNHX4* gene in the leaf (Gálvez et al., 2012), whereas in the present experiment, the greatest induction was in the *SlNHX8* gene in the open flower tissue (Figure 10). It has been previously reported that transgenic tomatoes overexpressing *LeNHX2* have increased salt tolerance (Huertas et al., 2013). This gene corresponds to the *SlNHX6* gene, which was significantly upregulated at all time intervals after salt shock treatment in the present study (Figure 10). These findings point to the importance of the *SlNHX6/LeNHX2* gene in improving salt stress tolerance in the tomato. Jabeen et al. (2022) reported that there was no change in the expression level of *HvNHX1* in the leaf tissue of the Gairdner barley cultivar under 300-mM NaCl compared with the control. A similar finding was observed for the expression pattern of the *SlNHX1* gene at all time points in the open flower tissue, except at 6 h (Figure 10). A previous report also showed that all members of *MtNHX* genes were also upregulated under salt stress in flower tissues in *M. truncatula* (Sandhu et al., 2018) although some differences in terms of gene expression levels stand out in flower tissues of *S. lycopersicum* and *M. truncatula* (Sandhu et al., 2018). For instance, the *SlNHX7* gene was highly expressed in flower tissue after 24 h, whereas low expression profile of *MtNHX7* gene was reported in flower tissue of *M. truncatula* (Sandhu et al., 2018). Conversely, the *BvNHX5/BvSOS* gene in *B. vulgaris* under salt stress was significantly upregulated in leaves (Wu et al., 2019). Moreover, it has been determined that *PgNHX* genes showed different functions depending on the tissue in pomegranate roots and leaves (Dong et al., 2021). Taken together, these results suggested that the expression patterns of orthologous genes of the *NHX* family in different plant species might differentially be tuned in response to salt stress based on severity of the stress and type of plant tissue.

5 | CONCLUSION

In this study, a total of seven *SlNHX* genes were identified, and the phylogenetic analysis provided three classes based on their subcellular localizations. Members of the *SlNHX* family were grouped with *SlNHX1–4* on vacuole membranes, *SlNHX6* on the endosomal region, and *SlNHX7–8* on the PM. The amiloride binding site domain [FFIYLLPPI] was fully conserved in *SlNHX1–3*, whereas this domain was highly conserved in *SlNHX4* and *SlNHX6*. The *cis*-acting element analysis revealed that *SlNHX6* and *SlNHX8* were involved with the stress-related hormone MeJA in response to salt stress signaling. The PPI network analysis results indicated that the proteins SlNHX7 and SlNHX8 hypothetically interacted with the CBL and CIPK pathway in salt stress response. The RT-qPCR analysis showed that all *SlNHX* genes in the open flower tissues were significantly upregulated under salt shock, although the expression pattern was time dependent. The results pointed out the importance of the *SlNHX* genes in relation to salinity stress tolerance in the tomato. Our results suggest that the *SlNHX* genes identified using the current tomato genome information provide novel reference genes for future studies on salt stress in the tomato.

AUTHOR CONTRIBUTIONS

I.T. conceived the idea, planned the experiments, interpreted the data, and designed the figures. U.S. and E.C. performed the bioinformatic analysis and RT-qPCR analysis and drafted the manuscript. All authors read and approved the manuscript.

ACKNOWLEDGMENTS

We would like to thank Dr. Martha Rowe for editing the revised version of the manuscript.

CONFLICT OF INTEREST STATEMENT

The authors declare that they have no conflict of interest.

DATA AVAILABILITY STATEMENT

Data sharing is not applicable to this article as no new data were created or analyzed in this study.

ORCID

Erman Cavusoglu https://orcid.org/0000-0002-5874-4286
Ugur Sari https://orcid.org/0000-0001-7564-997X
Iskender Tiryaki https://orcid.org/0000-0002-7504-2892

REFERENCES

Aharon, G. S., Apse, M. P., Duan, S., Hua, X., & Blumwald, E. (2003). Characterization of a family of vacuolar Na^+/H^+ *antiporters* in *Arabidopsis thaliana*. *Plant and Soil*, *253*, 245–256. https://doi.org/10.1023/A:1024577205697

Akram, U., Song, Y., Liang, C., Abid, M. A., Askari, M., Myat, A. A., Abbas, M., Malik, W., Ali, Z., Guo, S., Zhang, R., & Meng, Z. (2020). Genome-wide characterization and expression analysis of *NHX* gene family under salinity stress in *Gossypium barbadense* and its comparison with *Gossypium hirsutum*. *Genes (Basel)*, *11*, 1–22. https://doi.org/10.3390/genes11070803

Ashraf, M., & McNeilly, T. (2004). Salinity tolerance in Brassica oilseeds. *CRC. Critical Reviews in Plant Sciences*, *23*, 157–174. https://doi.org/10.1080/07352680490433286

Ayadi, M., Martins, V., Ben Ayed, R., Jbir, R., Feki, M., Mzid, R., Géros, H., Aifa, S., & Hanana, M. (2020). Genome wide identification, molecular characterization, and gene expression analyses of grapevine *NHX* antiporters suggest their involvement in growth, ripening, seed dormancy, and stress response. *Biochemical Genetics*, *58*, 102–128. https://doi.org/10.1007/s10528-019-09930-4

Babu, M. A., Singh, D., & Gothandam, K. M. (2012). The effect of salinity on growth, hormones and mineral elements in leaf and fruit of tomato cultivar PKM1. *Journal of Animal and Plant Sciences*, *22*, 159–164.

Bacha, H., Tekaya, M., Drine, S., Guasmi, F., Touil, L., Enneb, H., Triki, T., Cheour, F., & Ferchichi, A. (2017). Impact of salt stress on morpho-physiological and biochemical parameters of *Solanum lycopersicum* cv. Microtom leaves. *South African Journal of Botany*, *108*, 364–369. https://doi.org/10.1016/j.sajb.2016.08.018

Baghour, M., Akodad, M., Dariouche, A., Maach, M., el Haddaji, H., Moumen, A., Skalli, A., Venema, K., & Rodríguez-Rosales, M. P. (2023). Gibberellic acid and indole acetic acid improves salt tolerance in transgenic tomato plants overexpressing *LeNHX4* antiporter. *Gesunde Pflanz*, *75*, 687–693. https://doi.org/10.1007/s10343-022-00734-y

Baghour, M., Gálvez, F. J., Sánchez, M. E., Aranda, M. N., Venema, K., & Rodríguez-Rosales, M. P. (2019). Overexpression of *LeNHX2* and *SlSOS2* increases salt tolerance and fruit production in double transgenic tomato plants. *Plant Physiology and Biochemistry*, *135*, 77–86. https://doi.org/10.1016/j.plaphy.2018.11.028

Bailey, T. L., Johnson, J., Grant, C. E., & Noble, W. S. (2015). The MEME suite. *Nucleic Acids Research*, *43*, W39–W49. https://doi.org/10.1093/nar/gkv416

Bandeh-hagh, A., Toorchi, M., Mohammadi, A., Chaparzadeh, N., Salekdeh, G. H., & Kazemnia, H. (2008). Growth and osmotic adjustment of canola genotypes in response to salinity. J. Food. *Agriculture and Environment*, *6*, 201–208.

Bassil, E., Ohto, M., Esumi, T., Tajima, H., Zhu, Z., Cagnac, O., Belmonte, M., Peleg, Z., Yamaguchi, T., & Blumwald, E. (2011). The *Arabidopsis* intracellular Na^+/H^+ *antiporters NHX5* and *NHX6* are endosome associated and necessary for plant growth and development. *Plant Cell*, *23*, 224–239. https://doi.org/10.1105/tpc.110.079426

Berardini, T. Z., Reiser, L., Li, D., Mezheritsky, Y., Muller, R., Strait, E., & Huala, E. (2015). The *Arabidopsis* information resource: Making and mining the "gold standard" annotated reference plant genome. *Genesis*, *53*, 474–485. https://doi.org/10.1002/dvg.22877

Berman, H. M., Westbrook, J., Feng, Z., Gilliland, G., Bhat, T. N., Weissig, H., Shindyalov, I. N., & Bourne, P. E. (2000). The Protein Data Bank. *Nucleic Acids Research*, *28*, 235–242. https://doi.org/10.1093/nar/28.1.235

Blanc, G., & Wolfe, K. H. (2004). Widespread paleopolyploidy in model plant species inferred from age distributions of duplicate genes. *Plant Cell*, *16*, 1667–1678. https://doi.org/10.1105/tpc.021345

Brett, C. L., Donowitz, M., & Rao, R. (2005). Evolutionary origins of eukaryotic *sodium/proton exchangers*. *American Journal of Physiology - Cell Physiolog*, *288*, C223–C239. https://doi.org/10.1152/ajpcell.00360.2004

Chandna, R., Azooz, M. M., & Ahmad, P. (2013). Recent advances of metabolomics to reveal plant response during salt stress. In P. Ahmad, M. M. Azooz, & M. N. V. Prasad (Eds.), *Salt stress in plants: Signalling, omics and adaptations* (pp. 1–14). New York, NY: Springer. https://doi.org/10.1007/978-1-4614-6108-1_1

Chen, C., Chen, H., Zhang, Y., Thomas, H. R., Frank, M. H., He, Y., & Xia, R. (2020). TBtools: An integrative toolkit developed for interactive analyses of big biological data. *Molecular Plant*, *13*, 1194–1202. https://doi.org/10.1016/j.molp.2020.06.009

Chen, H. T., Chen, X., Wu, B. Y., Yuan, X. X., Zhang, H. M., Cui, X. Y., & Liu, X. Q. (2015). Whole-genome identification and expression analysis of K^+ *efflux antiporter* (*KEA*) and Na^+/H^+ *antiporter* (*NHX*) families under abiotic stress in soybean. *Journal of Integrative Agriculture*, *14*, 1171–1183. https://doi.org/10.1016/S2095-3119(14)60918-7

Choi, S. W., Hoshikawa, K., Fujita, S., Thi, D. P., Mizoguchi, T., Ezura, H., & Ito, E. (2018). Evaluation of internal control genes for quantitative realtime PCR analyses for studying fruit development of dwarf tomato cultivar 'Micro-Tom'. *Plant Biotechnology*, *35*, 225–235. https://doi.org/10.5511/plantbiotechnology.18.0525a

Chou, K. C., & Shen, H. B. (2010). Plant-mPLoc: A top-down strategy to augment the power for predicting plant protein subcellular localization. *PLoS ONE*, *5*, e11335. https://doi.org/10.1371/journal.pone.0011335

Chutipaijit, S., Cha-um, S., & Sompornpailin, K. (2011). High contents of proline and anthocyanin increase protective response to salinity in *Oryza sativa* L. spp. indica. *Australian Journal of Crop Science*, *5*, 1191–1198.

Clinton, S. K. (2005). Tomatoes or lycopene: A role in prostate carcinogenesis? *The Journal of Nutrition*, *135*, 2057S–2059S. https://doi.org/10.1093/jn/135.8.2057s

Cook, C. E., Bergman, M. T., Cochrane, G., Apweiler, R., & Birney, E. (2018). The European bioinformatics institute in 2017: Data coordination and integration. *Nucleic Acids Research*, *46*, D21–D29. https://doi.org/10.1093/nar/gkx1154

Counillon, L., Franchi, A., & Pouyssegur, J. (1993). A point mutation of the Na^+/H^+ *exchanger* gene (*NHE1*) and amplification of the mutated allele confer amiloride resistance upon chronic acidosis. *Proceedings of the National Academy of Sciences of the United States of America*, *90*, 4508–4512. https://doi.org/10.1073/pnas.90.10.4508

Cunningham, F., Allen, J. E., Allen, J., Alvarez-Jarreta, J., Amode, M. R., Armean, I. M., Austine-Orimoloye, O., Azov, A. G., Barnes, I., & Bennett, R. (2022). Ensembl 2022. *Nucleic Acids Research*, *50*, D988–D995. https://doi.org/10.1093/nar/gkab1049

Deinlein, U., Stephan, A. B., Horie, T., Luo, W., Xu, G., & Schroeder, J. I. (2014). Plant salt-tolerance mechanisms. *Trends in Plant Science*, *19*, 371–379. https://doi.org/10.1016/j.tplants.2014.02.001

Díez, M. J., & Nuez, F. (2008). Tomato. In *Vegetables II* (pp. 249–323). Springer. https://doi.org/10.1007/978-0-387-74110-9_7

Dong, J., Liu, C., Wang, Y., Zhao, Y., Ge, D., & Yuan, Z. (2021). Genome-wide identification of the *NHX* gene family in *Punica granatum* L. and their expressional patterns under salt stress. *Agronomy*, *11*, 264. https://doi.org/10.3390/agronomy11020264

Fernandez-Pozo, N., Menda, N., Edwards, J. D., Saha, S., Tecle, I. Y., Strickler, S. R., Bombarely, A., Fisher-York, T., Pujar, A., Foerster, H., Yan, A., & Mueller, L. A. (2015). The Sol Genomics Network (SGN)-from genotype to phenotype to breeding. *Nucleic Acids Research*, *43*, D1036–D1041. https://doi.org/10.1093/nar/gku1195

Fu, X., Lu, Z., Wei, H., Zhang, J., Yang, X., Wu, A., Ma, L., Kang, M., Lu, J., Wang, H., & Yu, S. (2020). Genome-wide identification and expression analysis of the *NHX* (*sodium/hydrogen antiporter*) gene family in cotton. *Frontiers in Genetics*, *11*, 964. https://doi.org/10.3389/fgene.2020.00964

Gálvez, F. J., Baghour, M., Hao, G., Cagnac, O., Rodríguez-Rosales, M. P., & Venema, K. (2012). Expression of *LeNHX* isoforms in response to salt stress in salt sensitive and salt tolerant tomato species. *Plant Physiology and Biochemistry*, *51*, 109–115. https://doi.org/10.1016/j.plaphy.2011.10.012

Gasteiger, E., Gattiker, A., Hoogland, C., Ivanyi, I., Appel, R. D., & Bairoch, A. (2003). ExPASy: The proteomics server for in-depth protein knowledge and analysis. *Nucleic Acids Research*, *31*, 3784–3788. https://doi.org/10.1093/nar/gkg563

Gaxiola, R. A., Rao, R., Sherman, A., Grisafi, P., Alper, S. L., & Fink, G. R. (1999). The *Arabidopsis thaliana* proton transporters, *AtNHX1* and *Avp1*, can function in cation detoxification in yeast. *Proceedings of the National Academy of Sciences*, *96*, 1480–1485. https://doi.org/10.1073/pnas.96.4.1480

Ghanem, M. E., Ghars, M. A., Frettinger, P., Pérez-Alfocea, F., Lutts, S., Wathelet, J. P., du Jardin, P., & Fauconnier, M. L. (2012). Organ-dependent oxylipin signature in leaves and roots of salinized tomato plants (*Solanum lycopersicum*). *Journal of Plant Physiology*, *169*, 1090–1101. https://doi.org/10.1016/j.jplph.2012.03.015

Ghanem, M. E., van Elteren, J., Albacete, A., Quinet, M., Martínez-Andújar, C., Kinet, J.-M., Pérez-Alfocea, F., & Lutts, S. (2009). Impact of salinity on early reproductive physiology of tomato (*Solanum lycopersicum*) in relation to a heterogeneous distribution of toxic ions in flower organs. *Functional Plant Biology*, *36*, 125–136. https://doi.org/10.1071/FP08256

Goodstein, D. M., Shu, S., Howson, R., Neupane, R., Hayes, R. D., Fazo, J., Mitros, T., Dirks, W., Hellsten, U., Putnam, N., & Rokhsar, D. S. (2012). Phytozome: A comparative platform for green plant genomics. *Nucleic Acids Research*, *40*, D1178–D1186. https://doi.org/10.1093/nar/gkr944

Halfter, U., Ishitani, M., & Zhu, J.-K. (2000). The *Arabidopsis* SOS2 protein kinase physically interacts with and is activated by the calcium-binding protein SOS3. *Proceedings of the National Academy of Sciences*, *97*, 3735–3740. https://doi.org/10.1073/pnas.97.7.3735

Hamamoto, S., Horie, T., Hauser, F., Deinlein, U., Schroeder, J. I., & Uozumi, N. (2015). HKT transporters mediate salt stress resistance in plants: From structure and function to the field. *Current Opinion in Biotechnology*, *32*, 113–120. https://doi.org/10.1016/j.copbio.2014.11.025

Hanada, K., Shiu, S. H., & Li, W. H. (2007). The nonsynonymous/synonymous substitution rate ratio versus the radical/conservative replacement rate ratio in the evolution of mammalian genes. *Molecular Biology and Evolution*, *24*, 2235–2241. https://doi.org/10.1093/molbev/msm152

Harrewijn, P. (1979). Potassium and plant health. *Netherlands Journal of Plant Pathology*, *85*, 82. https://doi.org/10.1007/bf02349770

Hosmani, P.S., Flores-Gonzalez, M., van de Geest, H., Maumus, F., Bakker, L. V., Schijlen, E., van Haarst, J., Cordewener, J., Sanchez-Perez, G., & Peters, S. (2019). An improved *de novo* assembly and annotation of the tomato reference genome using single-molecule sequencing, Hi-C proximity ligation and optical maps. biorxiv 767764.

Huang, L., Li, Z., Sun, C., Yin, S., Wang, B., Duan, T., Liu, Y., Li, J., & Pu, G. (2022). Genome-wide identification, molecular characterization, and gene expression analyses of honeysuckle *NHX* antiporters suggest their involvement in salt stress adaptation. *PeerJ*, *10*, e13214. https://doi.org/10.7717/peerj.13214

Huertas, R., Rubio, L., Cagnac, O., García-Sánchez, M. J., Alché, J. D. D., Venema, K., Fernández, J. A., & Rodríguez-Rosales, M. P. (2013). The K^+/H^+ *antiporter LeNHX2* increases salt tolerance by improving K^+ homeostasis in transgenic tomato. *Plant, Cell and Environment*, *36*, 2135–2149. https://doi.org/10.1111/pce.12109

Hussain, Z., Khan, H., Imran, M., Naeem, M. K., Shah, S. H., Iqbal, A., Ali, S. S., Rizwan, M., Ali, S., Muneer, M. A., Widemann, E., & Shafiq, S. (2022). *Cation/proton antiporter* genes in tomato: Genomic characterization, expression profiling, and co-localization with salt stress-related QTLs. *Agronomy*, *12*, 245. https://doi.org/10.3390/agronomy12020245

Jabeen, Z., Irshad, F., Hussain, N., Han, Y., & Zhang, G. (2022). *NHX*-type Na^+/H^+ *antiporter* gene expression under different salt levels and allelic diversity of *HvNHX* in wild and cultivated barleys. *Frontiers in Genetics*, *12*, 809988. https://doi.org/10.3389/fgene.2021.809988

Jensen, L. J., Kuhn, M., Stark, M., Chaffron, S., Creevey, C., Muller, J., Doerks, T., Julien, P., Roth, A., Simonovic, M., Bork, P., & von Mering, C. (2009). STRING 8—A global view on proteins and their functional interactions in 630 organisms. *Nucleic Acids Research*, *37*, D412–D416. https://doi.org/10.1093/nar/gkn760

Krogh, A., Larsson, B., von Heijne, G., & Sonnhammer, E. L. L. (2001). Predicting transmembrane protein topology with a hidden Markov model: Application to complete genomes. *Journal of Molecular Biology*, *305*, 567–580. https://doi.org/10.1006/jmbi.2000.4315

Lescot, M., Déhais, P., Thijs, G., Marchal, K., Moreau, Y., van De Peer, Y., Rouzé, P., & Rombauts, S. (2002). PlantCARE, a database of plant cis-acting regulatory elements and a portal to tools for *in silico* analysis of promoter sequences. *Nucleic Acids Research*, *30*, 325–327. https://doi.org/10.1093/nar/30.1.325

Letunic, I., & Bork, P. (2021). Interactive tree of life (iTOL) v5: An online tool for phylogenetic tree display and annotation. *Nucleic Acids Research*, *49*, W293–W296. https://doi.org/10.1093/nar/gkab301

Li, N., Wang, X., Ma, B., Du, C., Zheng, L., & Wang, Y. (2017). Expression of a *Na+/H+ antiporter* RtNHX1 from a recretohalophyte *Reaumuria trigyna* improved salt tolerance of transgenic *Arabidopsis thaliana*. *Journal of Plant Physiology*, *218*, 109–120. https://doi.org/10.1016/j.jplph.2017.07.015

Liu, H., Wang, K., Mei, Q., Wang, X., Yang, J., Ma, F., & Mao, K. (2023). Genome-wide analysis of the *Actinidia chinensis NHX* family and characterization of the roles of *AcNHX3* and *AcNHX7* in regulating salt tolerance in *Arabidopsis*. *Environmental and Experimental Botany*, *214*, 105477. https://doi.org/10.1016/j.envexpbot.2023.105477

Liu, J., Ishitani, M., Halfter, U., Kim, C.-S., & Zhu, J.-K. (2000). The *Arabidopsis thaliana SOS2* gene encodes a protein kinase that is required for salt tolerance. *Proceedings of the National Academy of Sciences*, *97*, 3730–3734. https://doi.org/10.1073/pnas.97.7.3730

Livak, K. J., & Schmittgen, T. D. (2001). Analysis of relative gene expression data using real-time quantitative PCR and the $2^{-\Delta\Delta CT}$ method. *Methods*, *25*, 402–408. https://doi.org/10.1006/meth.2001.1262

Luo, X., Yang, S., Luo, Y., Qiu, H., Li, T., Li, J., Chen, X., Zheng, X., Chen, Y., Zhang, J., Zhang, Z., & Qin, C. (2021). Molecular characterization and expression analysis of the Na^+/H^+ *exchanger* gene family in *Capsicum annuum* L. *Frontiers in Genetics*, *12*, 1547. https://doi.org/10.3389/fgene.2021.680457

Lynch, M., & Conery, J. S. (2000). The evolutionary fate and consequences of duplicate genes. *Science (80-.)*, *290*, 1151–1155. https://doi.org/10.1126/science.290.5494.1151

Maach, M., Baghour, M., Akodad, M., Gálvez, F. J., Sánchez, M. E., Aranda, M. N., Venema, K., & Rodríguez-Rosales, M. P. (2020). Overexpression of *LeNHX4* improved yield, fruit quality and salt tolerance in tomato plants (*Solanum lycopersicum* L.). *Molecular Biology Reports*, *47*, 4145–4153. https://doi.org/10.1007/s11033-020-05499-z

Maach, M., Rodríguez-Rosales, M. P., Venema, K., Akodad, M., Moumen, A., Skalli, A., & Baghour, M. (2021). Improved yield, fruit quality, and salt resistance in tomato co-overexpressing *LeNHX2* and *SlSOS2* genes. *Physiology and Molecular Biology of Plants*, *27*, 703–712. https://doi.org/10.1007/s12298-021-00974-8

Madrid-Espinoza, J., Salinas-Cornejo, J., & Ruiz-Lara, S. (2019). The *Rab-GAP* gene family in tomato (*Solanum lycopersicum*) and wild relatives: Identification, interaction networks, and transcriptional analysis during plant development and in response to salt stress. *Genes (Basel)*, *10*, 638. https://doi.org/10.3390/genes10090638

Mahajan, S., Pandey, G. K., & Tuteja, N. (2008). Calcium- and salt-stress signaling in plants: Shedding light on SOS pathway. *Archives of Biochemistry and Biophysics*, *471*, 146–158. https://doi.org/10.1016/j.abb.2008.01.010

Manishankar, P., Wang, N., Köster, P., Alatar, A. A., & Kudla, J. (2018). Calcium signaling during salt stress and in the regulation of ion homeostasis. *Journal of Experimental Botany*, *69*, 4215–4226. https://doi.org/10.1093/jxb/ery201

Marschner, H. (1995). *Mineral nutrition of higher plants* (2nd ed., pp. 6–78). London: Academic Press. https://doi.org/10.1016/b978-0-12-473542-2.x5000-7

Munns, R. (1993). Physiological processes limiting plant growth in saline soils: Some dogmas and hypotheses. *Plant, Cell & Environment*, *16*, 15–24. https://doi.org/10.1111/j.1365-3040.1993.tb00840.x

Munns, R., & Tester, M. (2008). Mechanisms of salinity tolerance. *Annual Review of Plant Biology*, *59*, 651–681. https://doi.org/10.1146/annurev.arplant.59.032607.092911

Nataraja, K. N., & Parvathi, M. S. (2016). Tolerance to drought stress in plants: Unravelling the signaling networks. *Drought Stress Tolerance in Plants*, *5*, 71–90. https://doi.org/10.1007/978-3-319-32423-4_3

Olías, R., Eljakaoui, Z., Li, J., de Morales, P. A., Marín-Manzano, M. C., Pardo, J. M., & Belver, A. (2009). The plasma membrane Na^+/H^+ *antiporter SOS1* is essential for salt tolerance in tomato and affects the partitioning of Na^+ between plant organs. *Plant, Cell and Environment*, *32*, 904–916. https://doi.org/10.1111/j.1365-3040.2009.01971.x

Pandolfi, C., Mancuso, S., & Shabala, S. (2012). Physiology of acclimation to salinity stress in pea (*Pisum sativum*). *Environmental and Experimental Botany*, *84*, 44–51. https://doi.org/10.1016/j.envexpbot.2012.04.015

Pardo, J. M., Cubero, B., Leidi, E. O., & Quintero, F. J. (2006). Alkali cation exchangers: Roles in cellular homeostasis and stress tolerance. *Journal of Experimental Botany*, *57*, 1181–1199. https://doi.org/10.1093/jxb/erj114

Parihar, P., Singh, S., Singh, R., Singh, V. P., & Prasad, S. M. (2015). Effect of salinity stress on plants and its tolerance strategies: A review. *Environmental Science and Pollution Research*, *22*, 4056–4075. https://doi.org/10.1007/s11356-014-3739-1

Qiu, Q. S., Guo, Y., Dietrich, M. A., Schumaker, K. S., & Zhu, J. K. (2002). Regulation of *SOS1*, a plasma membrane Na^+/H^+ *exchanger* in *Arabidopsis thaliana*, by *SOS2* and *SOS3*. *Proceedings of the National Academy of Sciences of the United States of America*, *99*, 8436–8441. https://doi.org/10.1073/pnas.122224699

Rodríguez-Rosales, M. P., Jiang, X., Gálvez, F. J., Aranda, M. N., Cubero, B., & Venema, K. (2008). Overexpression of the tomato K^+/H^+ *antiporter LeNHX2* confers salt tolerance by improving potassium compartmentalization. *The New Phytologist*, *179*, 366–377. https://doi.org/10.1111/j.1469-8137.2008.02461.x

Roy, A., Kucukural, A., & Zhang, Y. (2010). I-TASSER: A unified platform for automated protein structure and function prediction. *Nature Protocols*, *5*, 725–738. https://doi.org/10.1038/nprot.2010.5

Sandhu, D., Pudussery, M. V., Kaundal, R., Suarez, D. L., Kaundal, A., & Sekhon, R. S. (2018). Molecular characterization and expression analysis of the Na^+/H^+ *exchanger* gene family in *Medicago truncatula*. *Functional & Integrative Genomics*, *18*, 141–153. https://doi.org/10.1007/s10142-017-0581-9

Shabala, S., & Cuin, T. A. (2008). Potassium transport and plant salt tolerance. *Physiologia Plantarum*, *133*, 651–669. https://doi.org/10.1111/j.1399-3054.2007.01008.x

Shi, H., Ishitani, M., Kim, C., & Zhu, J. K. (2000). The *Arabidopsis thaliana* salt tolerance gene *SOS1* encodes a putative Na^+/H^+ *antiporter*. *Proceedings of the National Academy of Sciences of the United States of America*, *97*, 6896–6901. https://doi.org/10.1073/pnas.120170197

Shi, H., Lee, B., Wu, S. J., & Zhu, J. K. (2003). Overexpression of a plasma membrane Na^+/H^+ *antiporter* gene improves salt tolerance in *Arabidopsis thaliana*. *Nature Biotechnology*, *21*, 81–85. https://doi.org/10.1038/nbt766

Siltberg, J., & Liberles, D. A. (2002). A simple covarion-based approach to analyse nucleotide substitution rates. *Journal of Evolutionary Biology*, *15*, 588–594. https://doi.org/10.1046/j.1420-9101.2002.00416.x

Tamura, K., Stecher, G., & Kumar, S. (2021). MEGA11: Molecular evolutionary genetics analysis version 11. *Molecular Biology and Evolution*, *38*, 3022–3027. https://doi.org/10.1093/molbev/msab120

Tester, M., & Davenport, R. (2003). Na^+ tolerance and Na^+ transport in higher plants. *Annals of Botany*, *91*, 503–527. https://doi.org/10.1093/aob/mcg058

Tian, F., Chang, E., Li, Y., Sun, P., Hu, J., & Zhang, J. (2017). Expression and integrated network analyses revealed functional divergence of *NHX*-type Na^+/H^+ *exchanger* genes in poplar. *Scientific Reports*, *7*, 1–17. https://doi.org/10.1038/s41598-017-02894-8

Valiollah, R. (2013). Effect of salinity stress on yield, component characters and nutrient compositions in rapeseed (*Brassica napus* L.) genotypes. *Agricultura Tropica et Subtropica*, *46*, 58–63. https://doi.org/10.2478/ats-2013-0010

van Zelm, E., Zhang, Y., & Testerink, C. (2020). Salt tolerance mechanisms of plants. *Annual Review of Plant Biology*, *71*, 403–433. https://doi.org/10.1146/annurev-arplant-050718-100005

Venema, K., Belver, A., Marín-Manzano, M. C., Rodríguez-Rosales, M. P., & Donaire, J. P. (2003). A novel intracellular K^+/H^+ *antiporter* related to Na^+/H^+ *antiporters* is important for K^+ ion homeostasis in plants. *The Journal of Biological Chemistry*, *278*, 22453–22459. https://doi.org/10.1074/jbc.M210794200

Wang, Y., Tang, H., Debarry, J. D., Tan, X., Li, J., Wang, X., Lee, T. H., Jin, H., Marler, B., Guo, H., Kissinger, J. C., & Paterson, A. H. (2012). MCScanX: A toolkit for detection and evolutionary analysis of gene synteny and collinearity. *Nucleic Acids Research*, *40*, e49. https://doi.org/10.1093/nar/gkr1293

Wang, Y., Ying, J., Zhang, Y., Xu, L., Zhang, W., Ni, M., Zhu, Y., & Liu, L. (2020). Genome-wide identification and functional characterization of the *cation proton antiporter* (*CPA*) family related to salt stress response in radish (*Raphanus sativus* l.). *International Journal of Molecular Sciences*, *21*, 1–20. https://doi.org/10.3390/ijms21218262

Ward, J. M., Mäser, P., & Schroeder, J. I. (2009). Plant ion channels: Gene families, physiology, and functional genomics analyses. *Annual Review of Physiology*, *71*, 59–82. https://doi.org/10.1146/annurev.physiol.010908.163204

Weinl, S., & Kudla, J. (2009). The CBL-CIPK Ca^{2+}-decoding signaling network: Function and perspectives. *The New Phytologist*, *184*, 517–528. https://doi.org/10.1111/j.1469-8137.2009.02938.x

Wu, G. Q., Wang, J. L., & Li, S. J. (2019). Genome-wide identification of Na^+/H^+ *antiporter* (*NHX*) genes in sugar beet (*Beta vulgaris* L.) and their regulated expression under salt stress. *Genes (Basel)*, *10*, 401. https://doi.org/10.3390/genes10050401

Yamaguchi, T., Apse, M. P., Shi, H., & Blumwald, E. (2003). Topological analysis of a plant vacuolar Na^+/H^+ *antiporter* reveals a luminal C terminus that regulates antiporter cation selectivity. *Proceedings of*

the National Academy of Sciences of the United States of America, *100*, 12510–12515. https://doi.org/10.1073/pnas.2034966100

Yamaguchi, T., Hamamoto, S., & Uozumi, N. (2013). Sodium transport system in plant cells. *Frontiers in Plant Science*, *4*, 140–151. https://doi.org/10.3389/fpls.2013.00410

Yang, J., Roy, A., & Zhang, Y. (2013). Protein-ligand binding site recognition using complementary binding-specific substructure comparison and sequence profile alignment. *Bioinformatics*, *29*, 2588–2595. https://doi.org/10.1093/bioinformatics/btt447

Yang, J., & Zhang, Y. (2015). Protein structure and function prediction using I-TASSER. *Current Protocols in Bioinformatics*, *52*, 5.8.1–5.8.15. https://doi.org/10.1002/0471250953.bi0508s52

Zhang, M., Qin, Z., & Liu, X. (2005). Remote sensed spectral imagery to detect late blight in field tomatoes. *Precision Agriculture*, *6*, 489–508. https://doi.org/10.1007/s11119-005-5640-x

Zhang, P., Senge, M., & Dai, Y. (2017). Effects of salinity stress at different growth stages on tomato growth, yield, and water-use efficiency. *Communications in Soil Science and Plant Analysis*, *48*, 624–634. https://doi.org/10.1080/00103624.2016.1269803

Zhang, Y. (2008). I-TASSER server for protein 3D structure prediction. *BMC Bioinformatics*, *9*, 1–8. https://doi.org/10.1186/1471-2105-9-40

Zouine, M., Maza, E., Djari, A., Lauvernier, M., Frasse, P., Smouni, A., Pirrello, J., & Bouzayen, M. (2017). TomExpress, a unified tomato RNA-Seq platform for visualization of expression data, clustering and correlation networks. *The Plant Journal*, *92*, 727–735. https://doi.org/10.1111/tpj.13711

How to cite this article: Cavusoglu, E., Sari, U., & Tiryaki, I. (2023). Genome-wide identification and expression analysis of Na^+/H^+ *antiporter* (*NHX*) genes in tomato under salt stress. *Plant Direct*, *7*(11), e543. https://doi.org/10.1002/pld3.543